Hindawi
Journal of Electrical and Computer Engineering
Volume 2019, Article ID 6287970, 11 pages
https://doi.org/10.1155/2019/6287970

Research Article

Dual-Band High *Q*-Factor Complementary Split-Ring Resonators Using Substrate Integrated Waveguide Method and Their Applications

Mehdi Hamidkhani,[1] **Rasool Sadeghi**,[1] **and Mohamadreza Karimi**[2]

[1]*Department of Electrical Engineering, Dolatabad Branch, Islamic Azad University, Isfahan, Iran*
[2]*Department of Computer Engineering, Dolatabad Branch, Islamic Azad University, Isfahan, Iran*

Correspondence should be addressed to Mehdi Hamidkhani; mehdi.hamidkhani@gmail.com

Received 13 January 2019; Revised 20 June 2019; Accepted 3 July 2019; Published 9 September 2019

Academic Editor: Hector E. Nistazakis

In modern microwave telecommunication systems, especially in low phase noise oscillators, there is a need for resonators with low insertion losses and high *Q*-factor. More specifically, it is of high interest to design resonators with high group delay. In this paper, three novel dual-band complementary split-ring resonators (CSRRs) featuring high group delay etched on the waveguide surface by using substrate integrated waveguides are investigated and proposed. They are designed for a frequency range of 4.5–5.5 GHz. Group delay rates for the first, second, and third resonators were approximated as much as 23 ns, 293 ns, and 90 ns, respectively. We also proposed a new practical method to develop a wide tuning range SIW CSRR cavity resonator with a small tuning voltage in the second resonator, which leads to about 19% and 1% of tuning frequency band in the first and second bands, respectively. Finally, some of their applications in the design of filter, diplexer, and low phase noise oscillator will be investigated.

1. Introduction

Metamaterials indicate a paradigm in electromagnetic science and technology. These materials have numerous unparalleled microwave utilizations [1]. A prominent application may be for designing resonators. Researchers proposed the split-ring resonator (SRR) and its dual complementary split-ring resonator (CSRR) as a main component for synthesizing metamaterial microstrip lines with negative permittivity, supporting a forward-wave or backward-wave passband [2, 3].

Metamaterials were applied by selecting waveguide structures in this study. A reason for this is the increased *Q*-factor of the waveguide with a probable utilization for designing low loss and noise elements with acceptable power-handling ability. Another reason is the ability of the waveguide for providing negative permittivity when it is operated below the cutoff frequency of the dominant TE mode [3–6]. As CSRR exhibits negative permittivity, the use of CSRRs into waveguide conducing to a ε-positive material is a simple process. On the contrary, a forward-wave passband below the cutoff frequency would be obtained [4, 5].

We chose a substrate integrated waveguide (SIW) because combining CSRRs with a conventional metallic waveguide is hard. Of course, SIW has been one of the commonest types of planar guided wave structures during the previous years. Then, it was synthesized on a planar substrate with linear periodic arrays of metallic vias based on the printed circuit board (PCB) technology. SIW on PCB was implemented in the microwave and millimeter wave integrated circuits, including dividers, filters, couplers, circulators, multiport circuits, and antennas. Figure 1 depicts configuration of SIW. The relations below must be supported. The relations were necessary for filling all gaps in the design frequency band, declining the scattering loss, and ensuring easy construction. SIW enjoys acceptable properties, including low profile, affordability, and simple

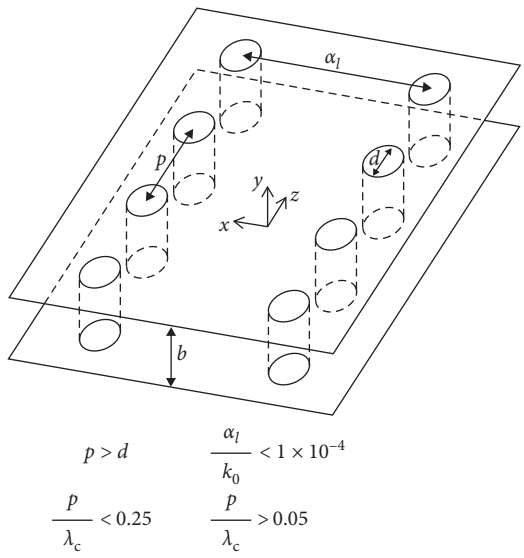

Figure 1: SIW technology.

incorporation with planar circuit. It also has advantages of the features of traditional rectangular waveguide. Most importantly, etching the CSRRs on the waveguide surface is done very easily by SIW [3–7].

Group delay is a significant property of the electrical and communication systems and instruments. It depends on the group delay of the system components. In addition, it is a criterion of the device phase distortion, transition duration of a signal via a tool versus frequency, and derivative of the tool phase property based on the frequency. Group delay is defined as the negative derivative of the DUT's phase characteristic against frequency [8]:

$$\tau_{\mathrm{d}} = -\frac{1}{360}\frac{d\varphi}{df}, \tag{1}$$

where τ_{d} represents the group delay, f refers to the frequency, and φ indicates S_{11} or S_{21} phase in degrees. It is possible that there is a relationship between the group delay and reflection coefficient, which is the devices group delay or transmission coefficient, which is the transmission (or insertion) group delay. Equation (2) produces external quality factor through the group delay of S_{11}, which is employed in singly loaded resonator, while the group delay of S_{21} is provided by equation (3), which is applied in a doubly loaded resonator [8].

$$Q_e = \frac{\omega_{\mathrm{o}} \cdot \tau_{S_{11}}(\omega_{\mathrm{o}})}{4}, \tag{2}$$

$$Q_e = \frac{\omega_{\mathrm{o}} \cdot \tau_{S_{21}}(\omega_o)}{2}, \tag{3}$$

where ω_{o} represents angular frequency.

The present study emphasized on the SIW loaded by the suggested CSRRs, which operate far below the initial waveguide cutoff frequency, resulting in a significant degree of miniaturization. We can design, fabricate, and measure 3 various kinds of resonators via making changes in the dimension and shape of the recommended CSRR. A number of certain properties such as less insertion loss, very good selectivity with compact size, and very great group delay causing an increased Q-factor distinguish between such structures. Ultimately, the study addressed a number of their utilizations for designing a slight low-loss narrow-band quad-band filter, a slight low-loss dual-band diplexer, and a low phase noise oscillator. Put differently, the study proposed resonators for designing a lower phase noise oscillator compared to additional documents with smaller sizes and just 1 transistor. Not less than 2 transistors are required for obtaining such a low level of phase noise. However, just 1 transistor was used and reached this low level in phase noise.

2. The Proposed Configuration

Figure 2(a) demonstrates the base layout employed in [3], where various initiatives have been proposed. There is a relationship between the layout and a SIW CSRR cavity resonator containing the substrate of Rogers RT/Duroid 5880 with a relative permittivity of 2.2, 0.508 mm thickness and loss tangent of 0.0009. SIW implements the electric side walls of the waveguide as 2 linear arrays of the metalized vias. For filling all gaps in the design frequency band, reducing the scattering loss, and ensuring a simple construction, these vias diameters and a center-to-center spacing were optimized to 0.8 mm and 1.4 mm values. A CSRR was assumed and engraved on the waveguide metal cover. We applied a 50 ohm microstrip feed line. The waveguide width is ~12 mm, resulting in the cutoff frequency of initial SIW at approximately 8.7 GHz.

Moreover, the width and length values of the waveguide, that is, SIW size, are expressed in 2 ways. (1) All decreases in the waveguide width resulted in higher cutoff frequency and miniaturization factor. Yet, such a situation just affects the coupling, whereas it largely influences the passband below the cutoff. (2) The waveguide length into the CSRR and input microstrip (L parameter in Figure 2) control the coupling. Additionally, higher waveguide length would have a growing impact on the amounts of loss. In particular, an interaction exists between lower loss and greater coupling during the waveguide length adulation, whereas the two affect possessing a resonator with a high Q-factor. Furthermore, changes in the values of the waveguide width and length do not have a significant impact on the passbands. However, increasing these 2 variables' values results in the lower cutoff frequency of the initial waveguide.

Figure 3 portrays transmission response of the suggested resonator as achieved by the simulation outputs with the help of Ansoft HFSS software package and the simulated circuit model outcomes, which will be expressed in Section 6. The observed forward-wave passband is situated below the cutoff frequency of the waveguide run by SIW technology, which results in miniaturizing the structure. Making changes in the resonance frequency may individually control the passband position. Numerous parameters influence the self-resonance frequency of the CSRR, e.g., split and slot length and slot width and length of other factors raised in the

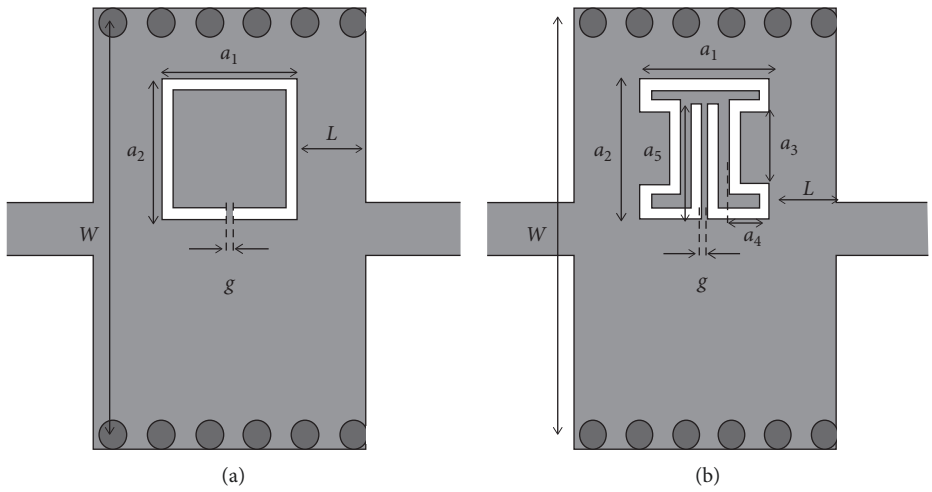

FIGURE 2: Configurations of (a) the base layout used in [3] and (b) the proposed base layout for SIW-CSRR unit cells [9].

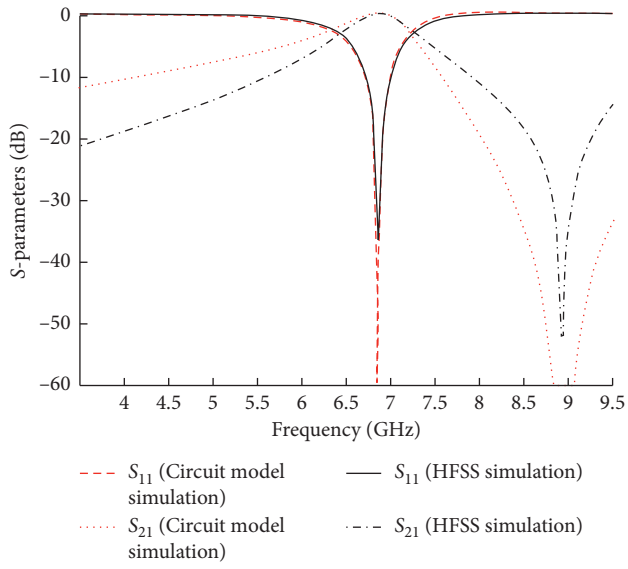

FIGURE 3: Simulated S-parameter responses corresponding to the unit cell shown in Figure 2(a). The geometrical parameters for the unit cells are $w = 12.3$ mm, $L = 2$ mm, $g = 0.18$ mm, $a_1 = 3.92$ mm, and $a_2 = 3.92$ mm. The electrical parameters of the equivalent circuit models in this case are $L_d = 0.9$ nH, $L_c = 0.6$ nH, $C_c = 0.5$ pF, $L_r = 1.15$ nH, and $C_r = 1$ pF [9].

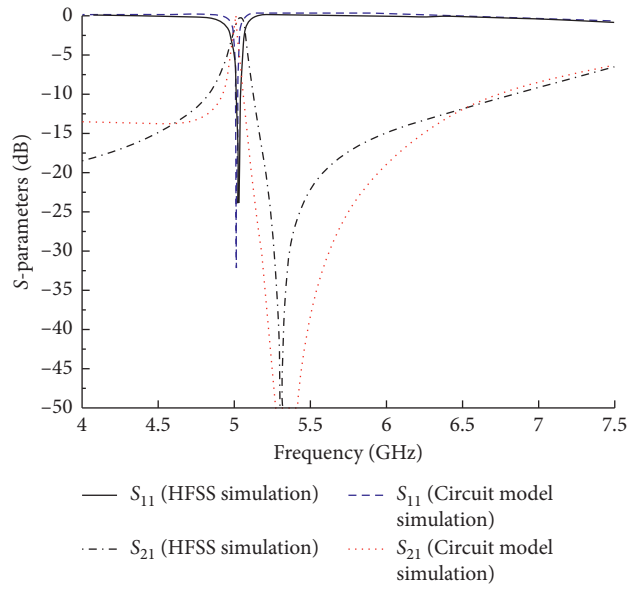

FIGURE 4: Simulated S-parameter responses corresponding to the unit cell shown in Figure 2(b). The geometrical parameters for the unit cells are $w = 12.3$ mm, $L = 2$ mm, $g = 0.18$ mm, $a_1 = 3.92$ mm, $a_2 = 3.92$ mm, $a_3 = 2$ mm, $a_4 = 1.2$ mm, and $a_5 = 3.2$ mm. The electrical parameters of the equivalent circuit models in this case are $L_d = 1.9$ nH, $L_c = 1.15$ nH, $C_c = 0.78$ pF, $L_r = 1.25$ nH, and $C_r = 1$ pF [9].

structure, which set the frequency. Hence, having a number of designs for additional frequency bands as the same as the ones proposed in the present study would be feasible. The study aimed at designing within the frequency range between 4.5 and 5.5 GHz.

Figure 2(b) shows the base layout suggested in the study, in which 3 high Q-factor resonators would be provided. The merely main difference in comparison to the layout recommended in [3] is that the alteration in the CSRR shape. Figure 4 depicts transmission response of the proposed base resonator and simulated circuit model outputs.

The two layouts have the same passband with 1 pole and 1 transmission zero situated above the passband, except for the situation that transmission zero is much closer to the pole for the suggested case, which results in the steep upper side transition, meaning that resonators with the recommended layout would possess greater group delays compared to the ones fabricated in [3], which ultimately results in greater quality factor and less noise structures. Figure 5 proves this situation by showing the group delay of both layouts.

One of the other merits of the suggested layout is that it provides the ground for us to attain a significantly increased miniaturization property. As seen, the frequency bandpass and group delay are nearly 6.8 GHz and 0.5 ns for the layout employed in [3] and 5.3 GHz and 4 ns for the layout recommended in the present study. Even though greater degrees of miniaturization and additional group delay can be

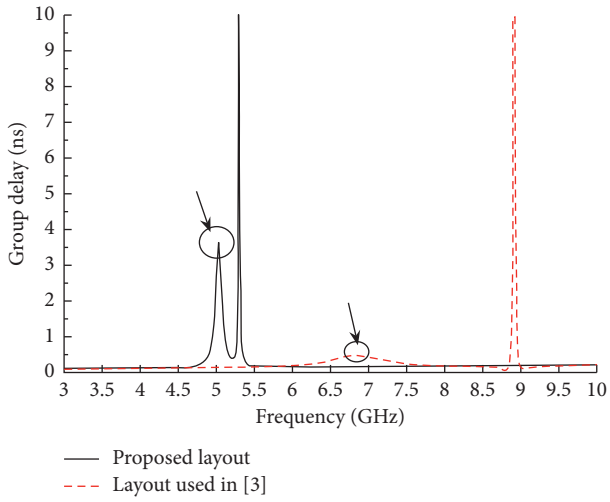

Figure 5: Simulated transmission group delay corresponding to the unit cells shown in Figures 2(a) and 2(b) [9].

achieved just if we cost higher insertion losses, this is possibly compensated via the use of active devices. Notably, the study aims at designing passive resonators. Moreover, active devices may be added to all structures below for achieving more group delay.

This section deals with the use of suggested layout and 3 high Q-factor resonators with various utilizations. The structures would be optimized in 2 frequency bands for gaining 3 objectives. (1) Achieving very high group delay over 20 ns with insertion loss lower than 2 dB not less than in 1 of the 2 frequency bands. (2) Designing a resonator working within functional frequency bands. (3) Achieving proximity of the 2 frequency bands for using them in utilizations, including self-oscillating mixer and low phase noise dual-band oscillator.

3. High Q-Factor Resonator 1

Figure 6(a) schematically draws the structure of the first suggested resonator and its optimized sizes [9]. According to the figure, it resembles the structure shown in Figure 2, except for a pair of nonevents suggested CSRRs would be chosen and imprinted on the waveguide metal cover, which results in the formation of 2 forward-wave passband below the cutoff frequency. The structure sizes would be configured in a way that the 2nd passband is situated between 2 poles. These conditions provided a ground for additional considerable increases in the group delay of the 2nd passband. Therefore, it allows achieving a high Q-factor resonator. Even though obtaining several group delays would be feasible, unfortunately it may lead to the corresponding higher side-effects via insertion loss.

Figures 7 and 8 show the simulated, measured, and circuit model outputs for transmission responses and group delay. The resonator contains 2 passbands at frequencies of ~4.7 GHz and 5.3 GHz. The group delay is 4 ns and 23 ns, which results in a total 0.5 dB and 2.1 dB insertion loss at the frequencies. Findings represent an external quality factor of ~383 and unloaded quality factor of ~1783 for the 2nd

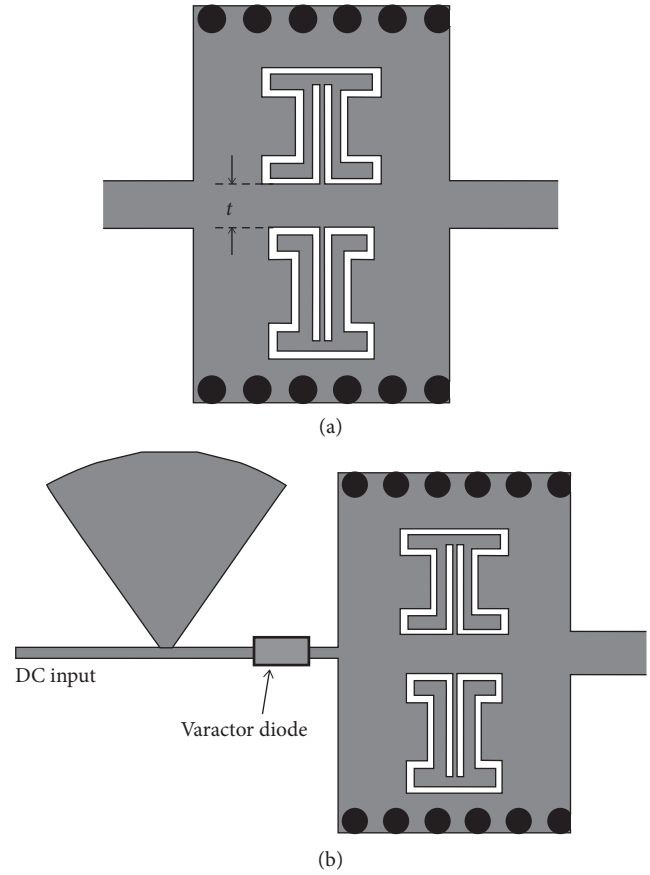

Figure 6: Configuration of the proposed resonators using proposed base layout: (a) first resonator [9] and (b) second resonator.

frequency band. Table 1 lists a summary of the comparisons between the recommended resonators and other published SIW BPFs. Similarly, this structure possesses benefits, including the compact size, lower insertion loss, higher return loss, and particularly higher Q-factor (higher group delay). Figure 9(a)shows the image of the constructed resonator. The structure may be applied in designing dual-band low phase noise parallel feedback-type oscillator.

4. High Q-Factor Resonator 2

Figure 6(b) shows the top view of the configuration of other SIW CSRR cavity resonators. It also consists of two metalized via arrays in the substrate of Rogers RT/Duroid 5880 and a pair of nonuniform CSRR are loaded on the metal cover of the waveguide. Illustration on the function of this structure is similar to that of the previous structure, which is based on the optimization of its dimensions. This structure has only one port, which can be used in the design of low phase noise serial feedback-type oscillator. Image for this fabricated resonator is shown in Figure 9(b).

In addition, this resonator is composed of a varactor diode which is a SMV1247 hyperabrupt junction tuning varactor. This is controlled by a dc voltage ranging from 0 to 4.7 V. The diode capacitance is about 7 pF at 0 V and 0.7 pF at 4.7 V. In fact, a practical approach of getting a wide tuning

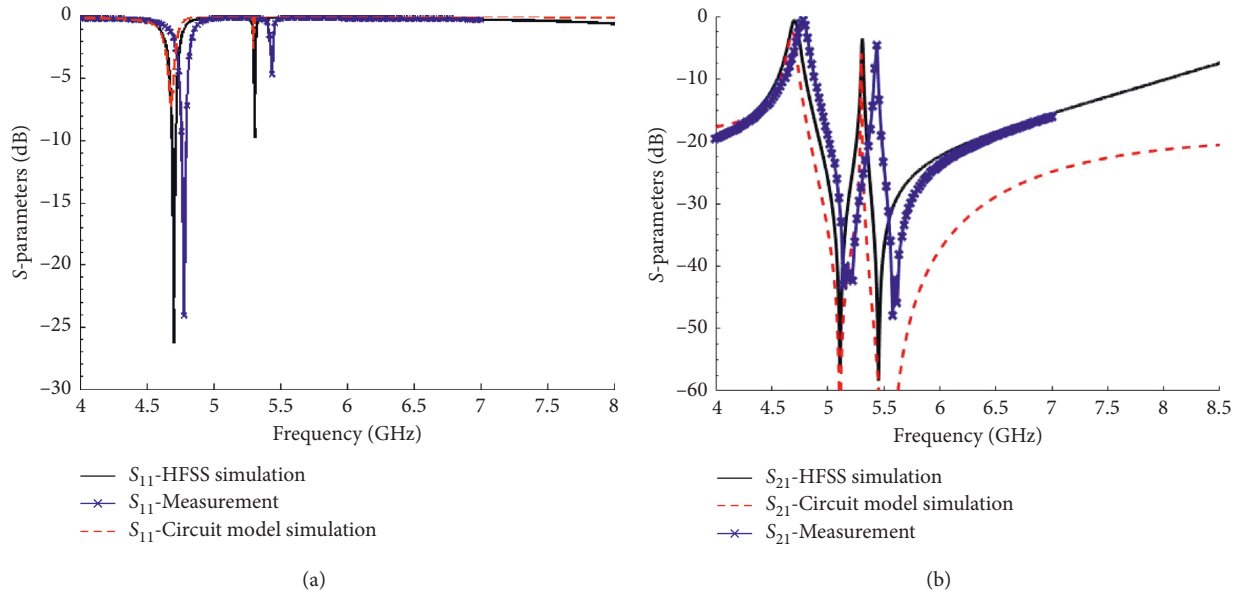

FIGURE 7: Measured and simulated transmission responses of the first proposed resonator. (a) S_{11} parameter and (b) S_{21} parameter. The geometrical parameters are $L = 2.2$ mm, $g = 0.2$ mm, $a_1 = 3.6$ mm, $a_2 = 3.6$ mm, $a_3 = 1.8$ mm, $a_4 = 1.2$ mm, and $a_5 = 3.1$ mm for the upper CSRR and $L = 2.4$ mm, $g = 0.2$ mm, $a_1 = 3.2$ mm, $a_2 = 4$ mm, $a_3 = 2$ mm, $a_4 = 0.9$ mm, and $a_5 = 3.5$ mm for the lower CSRR and $W = 11.5$ mm and $t = 1.3$ mm. The electrical parameters of the equivalent circuit models in this case are $L_d = 4$ nH, $L_c = 1$ nH, $C_c = 0.97$ pF, $L_s = 0.9$ nH, $C_s = 0.9$ pF, $L_{r1} = 1.35$ nH, $C_{r1} = 1.21$ pF, $L_{r2} = 0.65$ nH, and $C_{r2} = 1.52$ pF [9].

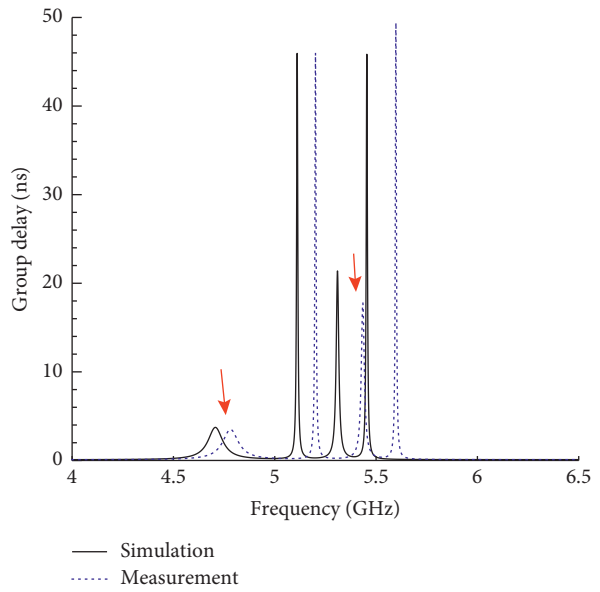

FIGURE 8: Simulated and measured transmission group delay corresponding to first proposed resonator [9].

range SIW CSRR cavity resonator given a small tuning voltage is presented that arises from the change in equivalent capacitance of the wall which is connected to the varactor diode.

The simulation result and measurement data show that the resonator 2 operates as a dual-band device. However, as expected, the second frequency band has a very high group delay. The varactor capacitance was swept using 0–4.7 V bias to find the widest tuning range, which leads to about 19% and 1% of tuning frequency band for the first and second band, respectively. Frequency response variations versus frequency for various values of the varactor diode capacitance can be seen in Figure 10. The effect of this bias on group delay can be seen in Table 2, that is, between 6–290 ns for all bias voltages. The results indicate a maximum external quality factor of approximately 2500 for the second frequency band. However, as mentioned, further group delay is at the cost of increased insertion losses, and in other words, decreased reflection coefficient, which partially can be compensated by using active devices.

5. High Q-Factor Resonator 3

The top view of the configuration of the third SIW CSRR cavity resonator is observed in Figure 11. The CSRR used in this section is similar to the previous sections other than the addition of a square annular gap, which allows for transmission zero to get closer to the pole at both frequency bands. Therefore, high group delay for both frequency bands can be achieved as compared to the previous structures. The results are shown in Figures 12–15, confirming the fact. In this section, two structures are proposed that one of them is fabricated and measured.

Owing to the high sensitivity of dimensions of this structure and high level of precision (as precise as 0.1 mm) required during its fabrication, it is natural to experience an incompatibility as high as what is seen in Figures 12 and 13 between the simulated and measured responses in structure (a). Interestingly, although here the precision in fabrication was around 0.2 mm, the obtained results were acceptable and the goals were achieved.

Table 1: Performance comparisons of the recent bandpass filter with the other.

Reference	No. of bands	Fractional bandwidth (%)	Insertion loss (dB)	Group delay (ns)	Size ($\lambda_0 \times \lambda_0$)
[3] (2-stage filter)	1	3.2	≅ 2	≅ 2	≅ 0.21 × 0.25
[10]	1	10.9	1.2	0.97	0.18 × 0.091
[11]	1	10.5	1.45	—	0.155 × 0.078
[12]	1	—	2.37	6.24	$0.129\lambda_g \times 0.094\lambda_g$
This work (first resonator)	2	0.2	0.5 & 2.1	4 & 23	0.21 × 0.1 (@5.3 GHz)

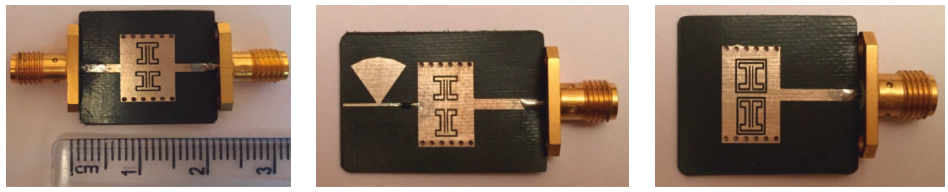

(a) (b) (c)

Figure 9: Images of the fabricated resonators.

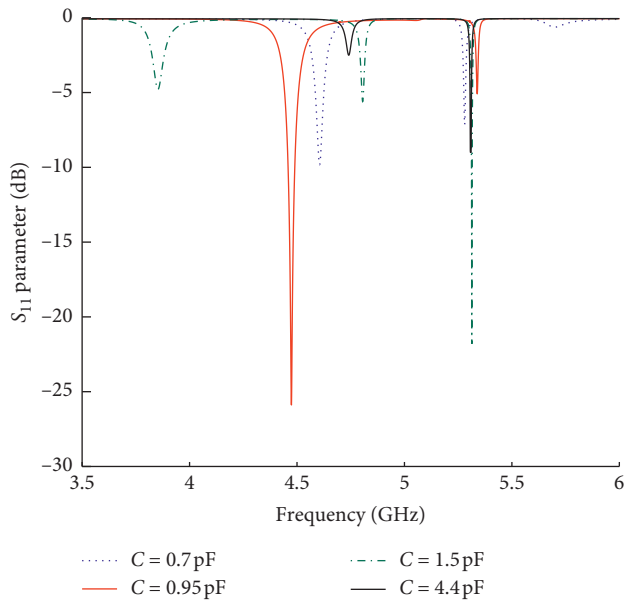

Figure 10: Frequency response variations of the second proposed resonator versus frequency for various values of the varactor diode capacitance. The geometrical parameters are $L = 2.2$ mm, $g = 0.2$ mm, $a_1 = 3.6$ mm, $a_2 = 3.6$ mm, $a_3 = 1.8$ mm, $a_4 = 1.2$ mm, and $a_5 = 3.1$ mm for the upper CSRR and $L = 2.4$ mm, $g = 0.2$ mm, $a_1 = 3.2$ mm, $a_2 = 4$ mm, $a_3 = 2$ mm, $a_4 = 0.9$ mm, and $a_5 = 3.5$ mm for the lower CSRR and $W = 11.5$ mm and $t = 1.3$ mm.

6. Equivalent Circuit Models

Equivalent circuit models were achieved and validated for design purposes and to realize the prominent differences between the unit cells. Figure 16 shows the circuit models of the suggested resonators when we ignored the material losses in the models. An inductance (L_d) as a short-circuited stub through the waveguide center may model SIW. CSRR would be modelled by the capacitance as the resonant tank and the inductance as the shunt-connected (L_r, C_r). L_c represents inductive connection basically across the ring split between waveguide transmission line and ring resonators. C_c refers to the capacitive coupling between CSRRs and waveguide transmission line. The coupling between waveguide and ring resonators depends on the waveguide length between CSRR and input microstrip, which is expressed by L in Figure 2. Put differently, if we increase this variable (L), it will result in greater coupling. Nonetheless, this also leads to higher losses along the waveguide transmission line. As mentioned earlier, we should address an interaction between higher coupling and higher losses for determining L value. With regard to the simulation outputs, the electric field reaches the highest level in the waveguide center for the recommended structures. Therefore, it provides a powerful coupling between waveguide and CSRRs.

Modelling of the coupling between the CSRRs would be performed as the resonant tank established by L_s and C_s that are inductive and capacitive couplings between CSRRs. Distance between the resonators would be adjusted to tune this coupling. The coupling would be more powerful in the case of the declined distance. Moreover, the waveguide width and CSRRs position may influence their coupling coefficient. It is possible to adjust such variables together so that a favorable coupling coefficient, group delay, and bandwidth are achieved for the passbands [3, 13].

Notably, the above circuit models are the versions with actual simplifications. Such simplification was caused by 3 reasons. (1) An inductance L_d shows the via-walls. It is necessary that infinite number of shunt inductances and the 2-wire transmission lines model them. (2) The CSRRs are coupled to the ground via a little capacitance C_2 and an equivalent inductance in a parallel manner. Impedance value of the parallel form would be much less than the value of SIW vias (L_d). Hence, we ignored impedance for simplifying the model. Actually, CSRR and ground were directly connected to each other. (3) We ignored the distributed shunt capacitance and distributed series inductance of the waveguide. Thus, the suggested circuit models would be valid just

Table 2: Frequency bands and group delay variations of the second proposed resonator for various values of varactor diode capacitance.

Varactor diode capacitance (pF)	Frequency bands (GHz)	Group delay of bands (ns)
0.3 (simulated)	4.668–5.35	16.4–161.5
0.7 pF@4.7 V (measured)	4.6–5.28	18.4–21.6
0.95 pF@3 V (measured)	4.47–5.34	60–16.6
1.1 (simulated)	4.324–4.931–5.322	7.8–6.3–101
1.5 (simulated)	3.853–4.806–5.314	2.8–31.8–254
2 (simulated)	4.769–5.311	23.5–250
4.4 pF@1 V (measured)	4.72–5.3	20–293
7 pF@0 V (measured)	4.72–5.3	19.5–205

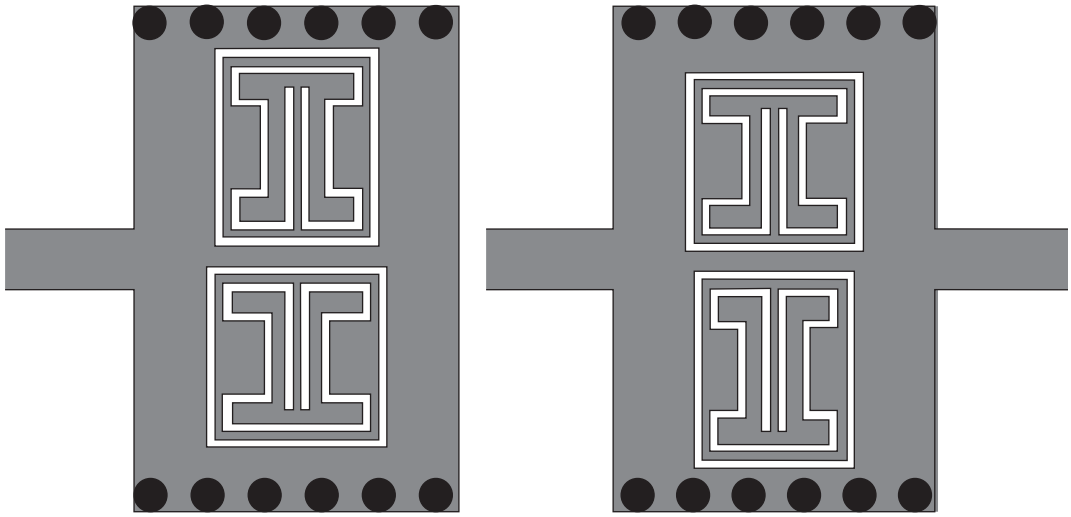

Figure 11: Configuration of the third proposed resonator using proposed base layout: (a) singly loaded resonator (one port) and (b) doubly loaded resonator (two ports).

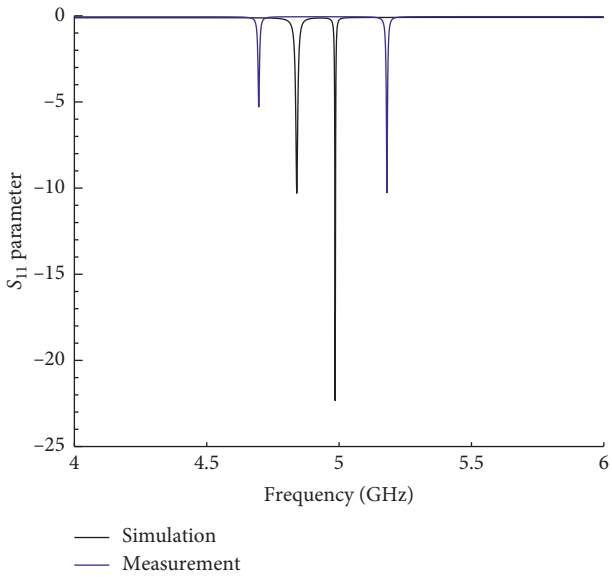

Figure 12: Measured and simulated frequency responses of third proposed resonator (structure a).

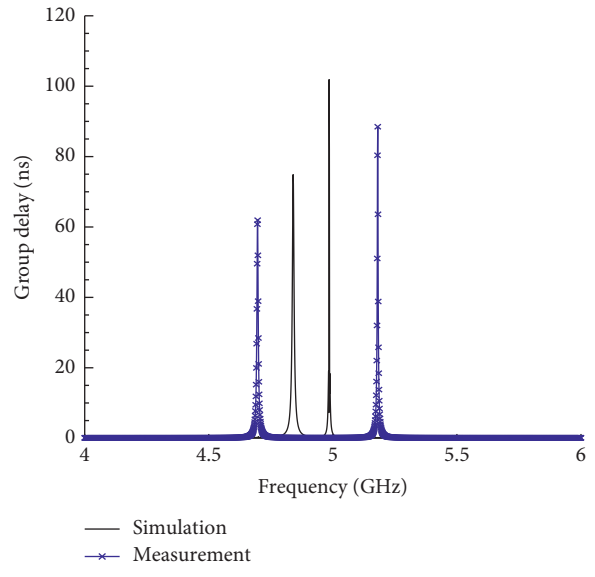

Figure 13: Measured and simulated group delay corresponding to the third proposed resonator (structure a).

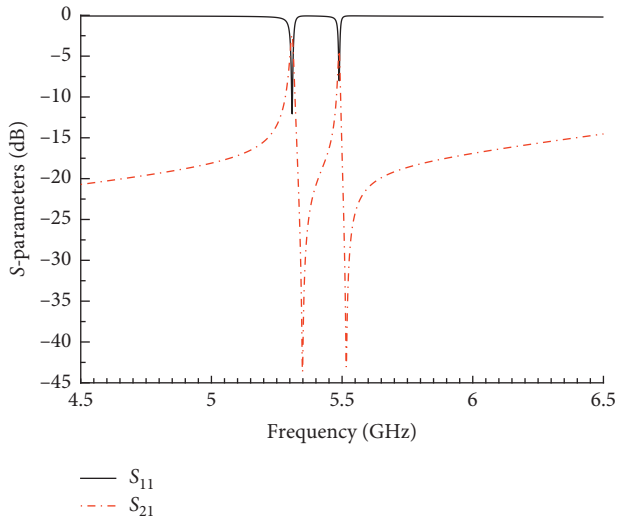

Figure 14: Simulated transmission responses of the third proposed resonator (structure b).

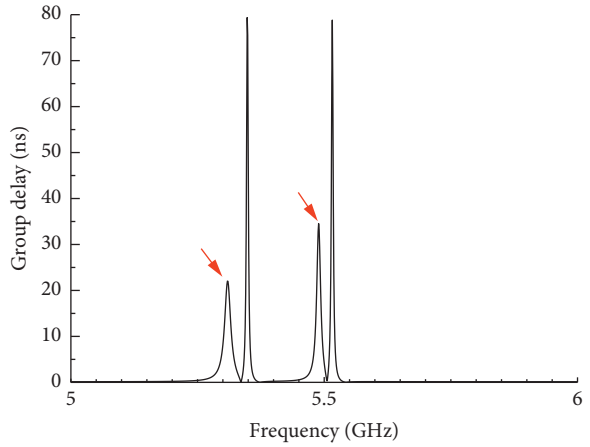

Figure 15: Simulated transmission group delay corresponding to the third proposed resonator (structure b).

for a certain frequency range. Nevertheless, they have a full ability to justify the transmission features of the structures [9].

7. Applications

These kinds of high Q-Factor resonators are significantly used in telecommunication and electronic communications. The compact multiband filter design is an example of such resonators [9]. Designing a convenient high-order filter through n aligned SIW-CSRRs would also be feasible. Such a situation allows the design of a filter with certain properties, whereas incorporation of the properties, including greater group delay, tuning of the band width, multiband, more selective passband with more acceptable out-of-band rejection, and greater degrees of freedom would be practicable. Nevertheless, it would be followed by greater insertion loss and relatively lower miniaturization. Figure 17 shows a sample made up of this filter. Figure 18 demonstrates the simulating and measuring outputs of the filter. It was revealed that passing bands in frequencies around 4.7, 5.3, 6.3, and 7.1 GHz would be accompanied by band width nearly 40, 8, 50, and 10 MHz while insertion losses would be nearly 0.6, 3.6, 1, and 2.5 decibels.

The compact multiband diplexer is another application [9]. It contains 3 ports and 2 continual filters that work below the cutoff frequency via SIW technology. T-junction was developed and optimized when 2 dual-band filters with favorable properties were achieved. Figure 19 indicates a sample fabricated of the above diplexer. Moreover, Figure 20 presents outputs of simulation and measurement. It was found that input signal passes through Port 1 to Port 3 with insertion loss stand at nearly 2.5 and 2.8 decibels in frequencies ~4.66 and 5.31 GHz. In addition, return loss stands at nearly 19 and 15 decibels. For frequencies around 6.36 and 7.17 GHz, input signal passes through Port 1 to Port 2 with insertion loss at nearly 1.8 and 3 decibels, while the return loss hits nearly 25 and 23.5 decibels. Moreover, each passband is isolated better in comparison with 25 decibels. Therefore, the suggested diplexer satisfies the criteria below: great miniaturizing percentage, increased isolation, less loss, and possible sending signals in 2 frequency bands in each route.

Designing low phase noise oscillator is one of the other prominent applications. The first phase of the suggested oscillator implementation is designing a high Q-factor resonator as explained in previous parts (the resonator suggested in Figure 6(b) in part 4 with high tuning abilities). It was assumed that the oscillator designing frequency is similar to the frequency of the suggested resonators, which had very high Q-factor and group delay. The second phase is designing an active device with ultra-low phase noise, which is unstable or has the potential of being unstable. Notwithstanding, active device provides the gain of the series feedback path that is a part of oscillation condition. ATF36077 was applied as the transistor in the above design. The corresponding transistor is an ultra-low noise transistor at band domain of 2–18 GHz. Figure 21 depicts an image of the constructed oscillator. Measurements demonstrated that oscillation frequency is equal to 5.33 GHz. The frequency adjustment range with varactor diode voltage changes would be nearly 81 MHz surrounding this oscillation frequency. Figure 22 draws the simulated (used in ADS software) and gauged phase noise at the oscillation frequency. There is a relative consistency between simulation and measurement outputs for the phase noise, except for the low offset frequency area, which may be caused by that exclusion of flicker noise source through the simulated oscillator. As shown, the 2 phase noises −129 dBc/Hz and −144 dBc/Hz were achieved at the offset frequency of 100 kHz and 1 MHz.

Table 3 makes a comparison between the suggested oscillator and additional planar microwave oscillators published somewhere else. This oscillator benefits in comparison with the ones stated in studies [14–17] are as follows: (1) other studies reported less phase noise as well as (2) this oscillator provides the ground for controlling oscillation frequency via making changes in the voltages. Put differently, it is possible to broadly tune the frequency passbands.

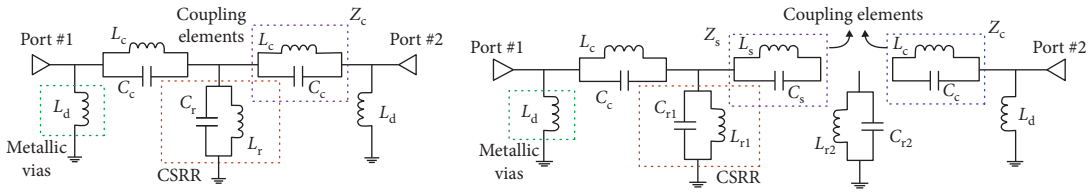

(a) (b)

FIGURE 16: (a) Equivalent circuit model for the base layouts introduced in Section 2. (b) Equivalent circuit corresponding to the first resonator.

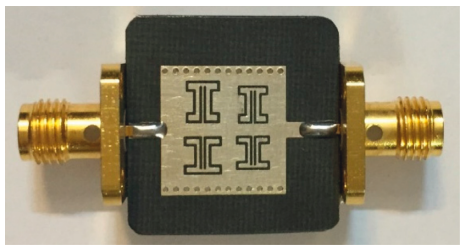

FIGURE 17: Image of the fabricated quad-band bandpass filter [9].

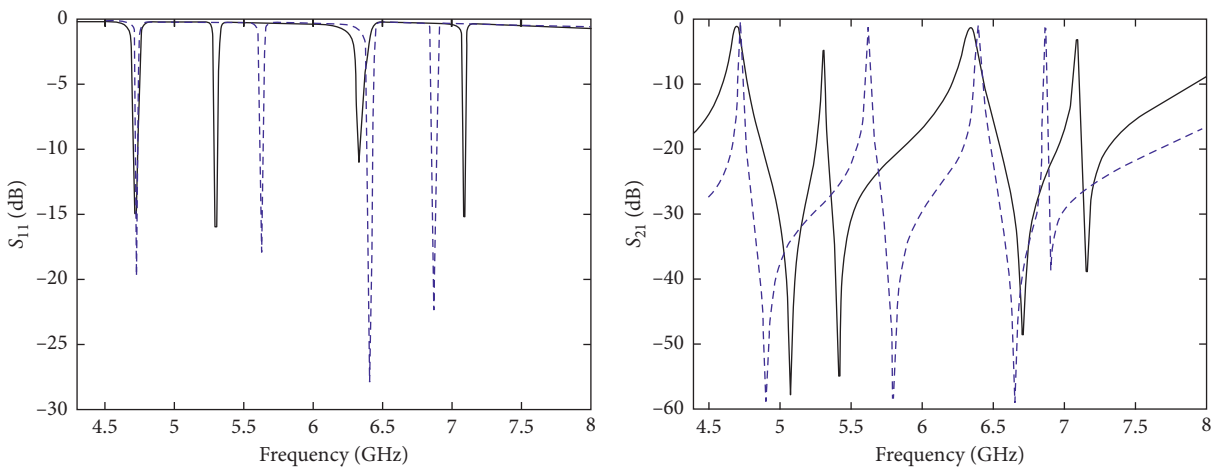

(a) (b)

FIGURE 18: Measured and simulated transmission responses of the proposed quad-band bandpass filter: (a) S_{11} parameter and (b) S_{21} parameter [9].

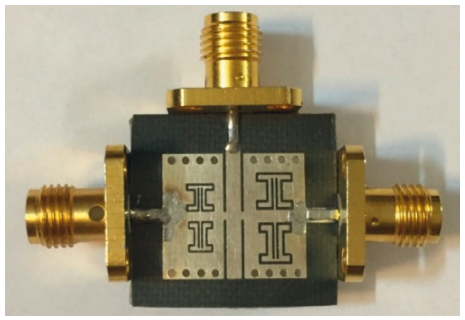

FIGURE 19: Image of the fabricated diplexer [9].

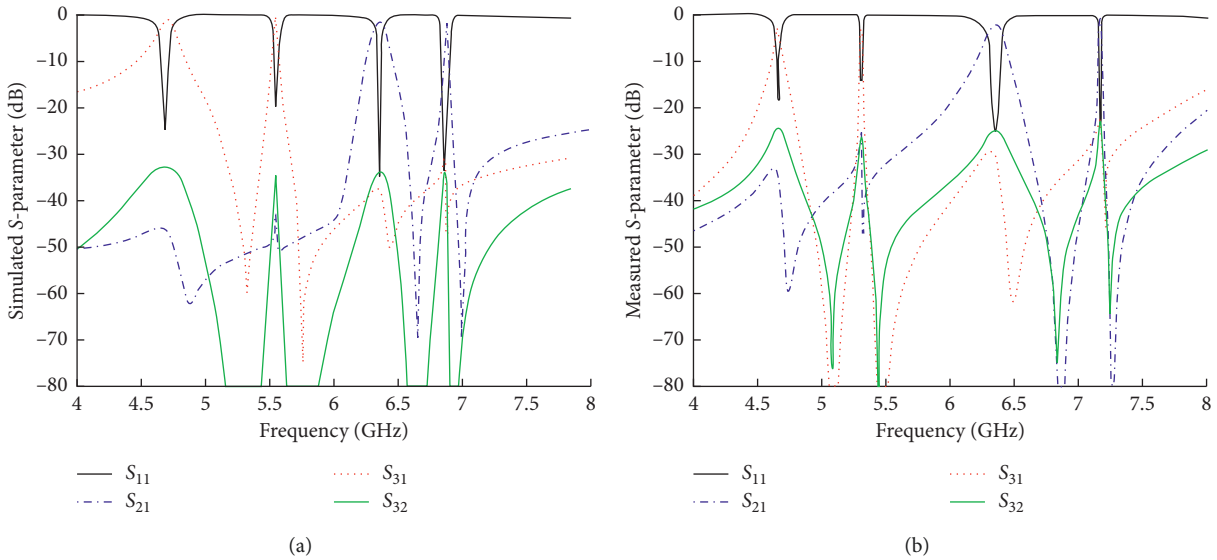

Figure 20: Measured and simulated transmission responses of the proposed diplexer [9].

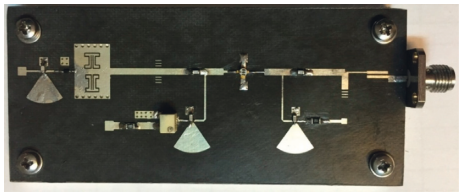

Figure 21: The circuit layout of the fabricated oscillator.

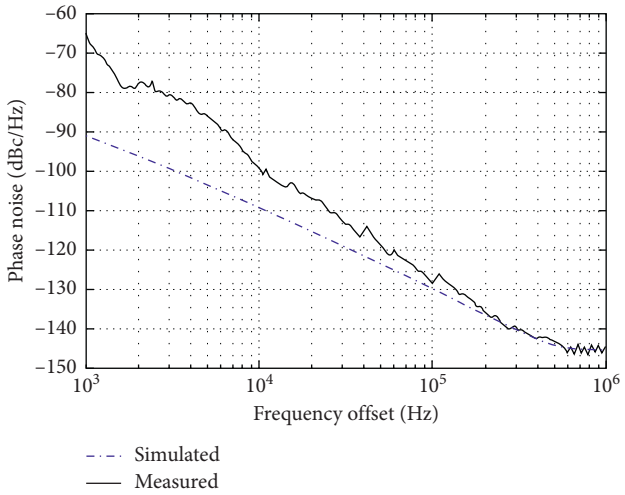

Figure 22: Measured and simulated phase noise for the proposed oscillator.

Table 3: Comparison with other reported microwave planar hybrid oscillator.

Ref.	Resonator	# of band	F_0 (GHz) (tuning)	P_output (dBm)	PN@100 kHz (dBc/Hz)
[14]	Cavity-backed CSRR	2	2.675 and 3.77	5.33 and 10.83	−105.5 and −99.63
[18]	SIW dual-mode filter	1	9	6.1	−111.9
[11]	SLNSRR	1	1.98	9.5	−127.22 (−145.43@1 MHz)
[19]	SIW cavity-backed CSRR	1	5.36	7	−128@100 kHz (−145@ 1 MHz)
Proposed oscillator (Figure 21)	SIW cavity-backed CSRR	1	5.33 (81 MHz)	8.6	−129 (−144@1 MHz)

8. Conclusion

In this paper, three novel dual-band passive high group delay complementary split-ring resonators (CSRRs) etched on the waveguide surface is proposed and fabricated. The group delay rate of about 23 ns, 293 ns, and 90 ns is accessible for the first, second, and third resonator, respectively. This is equivalent to a Q-factor of 383, 2500, and 750 for each structure. Then, a small low-loss narrow-band quad-band filter and a small low-loss dual-band diplexer with isolation better than 25 decibels are introduced and fabricated using this resonator. Also, we propose resonators in this paper to design a lower phase noise oscillator than other references with a smaller size and one only transistor.

Data Availability

The data used to support the findings of this study are available from the corresponding author upon request.

Conflicts of Interest

The authors declare that they have no conflicts of interest.

References

[1] C. Caloz and A. Rennings, "Overview of resonant metamaterial antennas," in *Proceedings of the 2009 3rd European Conference on Antennas and Propagation (EuCAP)*, Berlin, Germany, March 2009.

[2] J. D. Baena, J. Bonache, F. Martin et al., "Equivalent-circuit models for split-ring resonators and complementary split-ring resonators coupled to planar transmission lines," *IEEE Transactions on Microwave Theory and Techniques*, vol. 53, no. 4, pp. 1451–1461, 2005.

[3] D. D. Yuan, T. Yang, and T. Itoh, "Substrate integrated waveguide loaded by complementary split-ring resonators and its applications to miniaturized waveguide filters," *IEEE Transactions on Microwave Theory and Techniques*, vol. 57, no. 9, pp. 2211–2223, 2009.

[4] X.-C. Zhang, Z.-Y. Yu, and J. Xu, "Novel band-pass substrate integrated waveguide (SIW) filter based on complementary split ring resonators (CSRRs)," *Progress in Electromagnetics Research*, vol. 72, pp. 39–46, 2007.

[5] Y. Dong and T. Itoh, "Miniaturized dual-band substrate integrated waveguide filters using complementary split-ring resonators," in *Proceedings of the 2011 IEEE MTT-S International Microwave Symposium*, Baltimore, MD, USA, June 2011.

[6] Q.-L. Zhang, W.-Y. Yin, S. He, and L.-S. Wu, "Evanescent-mode substrate integrated waveguide (SIW) filters implemented with complementary split ring resonators," *Progress in Electromagnetics Research*, vol. 111, pp. 419–432, 2011.

[7] Y. Dong and T. Itoh, "Miniaturized substrate integrated waveguide slot antennas based on negative order resonance," *IEEE Transactions on Antennas and Propagation*, vol. 58, no. 12, pp. 3856–3864, 2010.

[8] J.-S. G. Hong and M. J. Lancaster, *Microstrip Filters for RF/microwave Applications*, John Wiley & Sons, Inc., Hoboken, NJ, USA, 2001.

[9] M. Hamidkhani and F. Mohajeri, "Dual-band complementary split-ring resonator (CSRR) with high-quality factor and its applications in low phase noise oscillators and small multi-band diplexers and filters," *Progress in Electromagnetics Research*, vol. 52, pp. 33–44, 2016.

[10] M. Danaeian, K. Afrooz, A. Hakimi, and A. R. Moznebi, "Compact bandpass filter based on SIW loaded by open complementary split-ring resonators," *International Journal of RF and Microwave Computer-Aided Engineering*, vol. 26, no. 8, pp. 674–682, 2016.

[11] M. Danaeian and H. Ghayoumi-Zadeh, "Miniaturized substrate integrated waveguide filter using fractal open complementary split-ring resonators," *International Journal of RF and Microwave Computer-Aided Engineering*, vol. 28, no. 5, article e21249, 2018.

[12] Z. Cai, Y. Liu, X. Tang, and T. Zhang, "A novel low phase noise oscillator using stubs loaded nested split-ring resonator," *IEEE Microwave and Wireless Components Letters*, vol. 27, no. 4, pp. 386–388, 2017.

[13] D. R. Chowdhury, R. Singh, A. J. Taylor, H. T. Chen, W. Zhang, and A. K. Azad, "Coupling schemes in terahertz planar metamaterials," *International Journal of Optics*, vol. 2012, Article ID 148985, 12 pages, 2012.

[14] Y. Dong and T. Itoh, "A dual-band oscillator with reconfigurable cavity-backed complementary split-ring resonator," in *Proceedings of the 2012 IEEE/MTT-S International Microwave Symposium Digest*, Montreal, Canada, June 2012.

[15] C.-L. Chang and C.-H. Tseng, "Design of low phase-noise oscillator and voltage-controlled oscillator using microstrip trisection bandpass filter," *IEEE Microwave and Wireless Components Letters*, vol. 21, no. 11, pp. 622–624, 2011.

[16] J. Choi, M. Nick, and A. Mortazawi, "Low phase-noise planar oscillators employing elliptic-response bandpass filters," *IEEE Transactions on Microwave Theory and Techniques*, vol. 57, no. 8, pp. 1959–1965, 2009.

[17] M. Nick and A. Mortazawi, "Oscillator phase-noise reduction using low-noise High-Q active resonators," in *Proceedings of the 2010 IEEE MTT-S International Microwave Symposium*, Anaheim, CA, USA, May 2010.

[18] Z. Yang, B. Luo, T. Yang, and J. Dong, "X-band low-phase noise oscillator employing substrate integrated waveguide dual-mode filter," *Electronics Letters*, vol. 51, no. 6, pp. 494-495, 2015.

[19] M. Hamidkhani and F. Mohajeri, "A low phase noise microwave oscillator based on a high Q SIW cavity CSRR bandpass filter," *Journal of Electromagnetic Waves and Applications*, vol. 30, no. 16, pp. 2077–2087, 2016.